A FOUR-ELEMENT ADAPTIVE ANTENNA ARRAY FOR IS-136 PCS BASE STATIONS

Robert L. Cupo, Glenn D. Golden**, Carol C. Martin*, Karl L. Sherman**, Nelson R. Sollenberger*, Jack H. Winters*, and Peter W. Wolniansky****

*** AT&T Labs - Research**
**** Lucent Technologies - Bell Labs**
Holmdel, New Jersey 07733 USA

Abstract: **We describe the algorithms, implementation, and laboratory performance of a real-time four element adaptive antenna array testbed for the uplink of a 1.9 GHz IS-136 PCS base station. Using our enhanced Direct Matrix Inversion algorithm, experimental results show nearly a 6 dB higher gain at a 10^{-2} bit error rate (BER) with four versus the typical two receive antennas and operation at close to a 10^{-2} BER even with an interferer of equal strength to the desired signal at 60 mph fading rates. These results demonstrate the feasibility of using adaptive arrays to increase both the range and capacity of TDMA cellular systems.**

I. INTRODUCTION

Antenna arrays using optimum combining reduce multipath fading of the desired signal and suppress interfering signals, thereby increasing both the range and capacity of wireless systems.

Previous work [1-3] has shown the potential improvement in gain and interference suppression using adaptive arrays in the TDMA mobile radio system IS-54/136. Computer simulation results [1] for a two-antenna array showed that, using the Direct Matrix Inversion (DMI) weight generation algorithm, the array could achieve significant increases in range and capacity with less than 1 dB loss from theoretically achievable gain due to weight tracking degradation at vehicle speeds up to 60 mph at 900 MHz. However, this paper did not consider other implementation issues such as errors in the data-derived reference signal, and recent interest has been focussed towards more antennas and PCS (1.9 GHz) frequencies, which causes increased tracking degradation (see, e.g., [2]).

In this paper, we study the performance of a four-element adaptive array intended for use on the uplink of an IS-136 PCS base station at 1.9 GHz. We present computer simulation results for the tracking performance of the DMI algorithm as presented in [1] and propose enhancements to that algorithm to improve tracking performance. We then briefly describe the implementation of a real-time adaptive array testbed, and show experimental results obtained with this testbed using an RF multipath fading emulator.

II. WEIGHT GENERATION ALGORITHMS

Figure 1 shows a block diagram of an M antenna element adaptive array. The complex baseband signal received by the ith element in the kth symbol interval $x_i(k)$ is multiplied by a controllable complex weight $w_i(k)$. The weighted signals are then summed to form the array output $y(k)$. Thus, the output signal is given by

$$y(k) = \mathbf{w}^T(k)\mathbf{x}(k) \quad , \tag{1}$$

where the weight vector $\mathbf{w}$ is given by

$$\mathbf{w} = \left[w_1 w_2 \cdots w_M\right]^T \quad , \tag{2}$$

the superscript T denotes transpose, and the received signal vector $\mathbf{x}$, which consists of the desired signal, thermal noise, and interference, is given by

$$\mathbf{x} = \left[x_1 x_2 \cdots x_M\right]^T \quad . \tag{3}$$

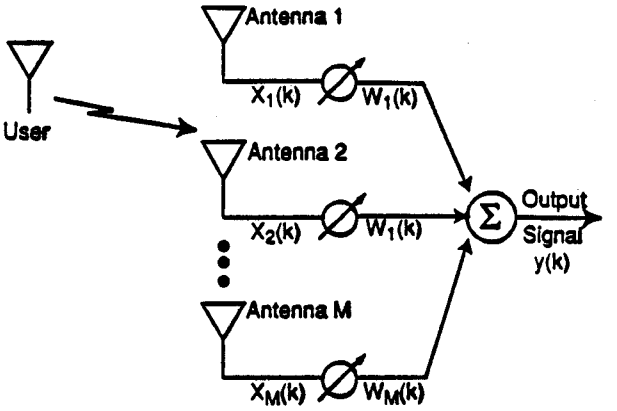

Fig. 1 Block diagram of an M element adaptive array.

The weights that minimize the mean squared error in the output signal, where the error is the difference between the output signal $y(k)$ and a reference signal $d(k)$, which ideally is the transmitted data (which also maximizes the signal-to-interference-plus-noise ratio (SINR) and minimizes the bit error rate (BER) with Gaussian noise), are given by [4],

$$\mathbf{w}(k) = \mathbf{R}_{xx}^{-1}(k)\mathbf{r}_{xd}(k) \quad . \tag{4}$$

In (4),

0-7803-3659-3/97 $10.00 ©1997 IEEE

$$\mathbf{R}_{xx} = E\left[\mathbf{x}^*\mathbf{x}^T\right] = \mathbf{u}_d^*\mathbf{u}_d^T + \sigma^2\mathbf{I} + \sum_{j=1}^{L} \mathbf{u}_j^*\mathbf{u}_j^T \quad , \qquad (5)$$

(assuming the desired signal, noise, and interfering signals are uncorrelated), where $\mathbf{u}_d$ and $\mathbf{u}_j$ are the desired and jth interfering signal propagation vectors, respectively, σ^2 is the noise power, $\mathbf{I}$ is the identity matrix, L is the number of interferers, and

$$\mathbf{r}_{xd}(k) = E[\mathbf{x}(k)d^*(k)] = \mathbf{u}_d \quad . \qquad (6)$$

Let us now consider the implementation of optimum combining using DMI as in [1]. Using a K-symbol rectangular averaging window, the weights are given by

$$\mathbf{w}(k+1) = \hat{\mathbf{R}}_{xx}^{-1}(k)\hat{\mathbf{r}}_{xd}(k) \qquad (7)$$

where

$$\hat{\mathbf{R}}_{xx}(k) = \frac{1}{K}\sum_{j=k-K+1}^{k} \mathbf{x}^*(j)\mathbf{x}^T(j) \quad , \qquad (8)$$

and

$$\hat{\mathbf{r}}_{xd}(k) = \frac{1}{K}\sum_{j=k-K+1}^{k} \mathbf{x}(j)d^*(j) \quad . \qquad (9)$$

Figure 2 shows the frame and time slot structure used in IS-136. For uplink (mobile to base) transmission, each time slot includes a 14 symbol synchronization sequence, and 6 symbol CDVCC sequence [5]. The synchronization sequence is intended for use in acquiring initial tap weight settings for an adaptive equalizer, while the CDVCC sequence identifies the mobile's associated base station. Both of these fields are known at the base station, and thus it is convenient to utilize them for adaptive array weight acquisition as well. Specifically, we use the synchronization sequence as the reference signal for initial weight acquisition, and then use the coherently-sliced detected data as the reference signal thereafter, i.e.,

$$d(k) = quan(\mathbf{w}^T(k)\mathbf{x}(k)) \qquad (10)$$

where $quan(\,)$ denotes $\pi/4$ QPSK coherent detection. Note that we consider coherent detection for the reference signal, but differential detection for the base station. This impacts performance as described below.

The performance obtained using DMI (7) is worse than that with the ideal weights (4) because of three factors: data detection errors, channel variation over the finite window, and noisy estimates for $\mathbf{R}_{xx}$ and $\mathbf{r}_{xd}$ with the finite window. Note that the effect of channel variation is reduced by decreasing K, while the effect of noisy estimates is reduced by increasing K. Fortunately, the best performance in IS-136 with 4 antennas is achieved with $K \simeq 14$, the length of the synchronization sequence. However, because of these effects, DMI has significantly degraded performance compared to ideal with 4 antennas in IS-136, particularly at high fading rates. Specifically, with noise only, the required signal-to-noise ratio (S/N) for a 10^{-2} BER is increased by 1.2 and 2.7 dB at 0 and 184 Hz (corresponding to 60 mph at 1.9 GHz), respectively, which is nearly half (in dB) the 6 dB theoretical gain one would achieve by going from 2 to 4 antennas. Furthermore, the loss is even greater with interference, as shown in the computer simulation results of Figure 3 for an equal-power interferer (i.e., signal-to-interference ratio, S/I = 0 dB) with 0, 92, and 184 Hz fading. (These curves are not smooth because of the BER measurement error with computer simulation using only 178 time slots.) With DMI, the required S/N for a 10^{-2} BER is increased by 2.1 and 11 dB at 0 and 184 Hz, respectively.

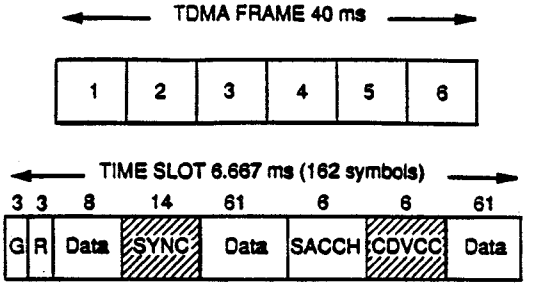

Fig. 2 The TDMA frame and time slot structure for IS-136.

To reduce this degradation we propose the following techniques. First, since DMI is based on optimum combining, this algorithm uses equal weighting for interference and noise suppression in the weight calculation. However, the estimate of the interference can be poorer than the estimate of the noise variance (which is typically known or can be accurately estimated). Thus, equal weighting of the noise and interference may not give the weights which result in lowest BER. Indeed, when interference is not present, our computer simulations and real-time experiments using a fading emulator show significant improvement when maximal ratio combining (MRC), which ignores interference, is used.

An enhancement to DMI which accommodates an adjustable relationship between the effects of noise and interference is diagonal loading (DMI/DL) (also known as "diagonal augmentation", and "eigenvalue shifting" [6]). The weights are given by

$$\mathbf{w}(k+1) = [(1-\beta)\hat{\mathbf{R}}_{xx}(k) + \beta\sigma^2\mathbf{I}]^{-1}\hat{\mathbf{r}}_{xd}(k) \quad , \qquad (11)$$

where the constant $\beta \leq 1$ is the diagonal loading factor.

As verified by our results, when the interference-to-noise ratio (I/N) is very large, $\beta = 0$, i.e., (7), gives the lowest BER, while when I/N is very small, $\beta = 1$, i.e., MRC, gives the lowest BER. However, most importantly, our results show that for I/N's between these values, there exist intermediate values of β's which give lower BER than either (7) or MRC, with the largest improvement over (7) and MRC when the interference and noise powers are comparable. Our results also show that the optimum β (for lowest BER) is nearly independent of S/N, although it does depend on the fading rate. Therefore, let us define β_{opt} as the β which results in the lowest BER in the presence of worst case fading, i.e., 184 Hz. Our results indicate that an appropriate choice for β_0 as a function of I/N (in dB) is

$$\beta_{opt} = \begin{cases} 1 & I/N \le -10 \\ \dfrac{20 - I/N}{30} & -10 < I/N \le 5 \\ .5 & 5 < I/N \le 8 \\ \dfrac{23 - I/N}{30} & 8 < I/N \le 23 \\ 0 & 23 < I/N \end{cases} \quad (12)$$

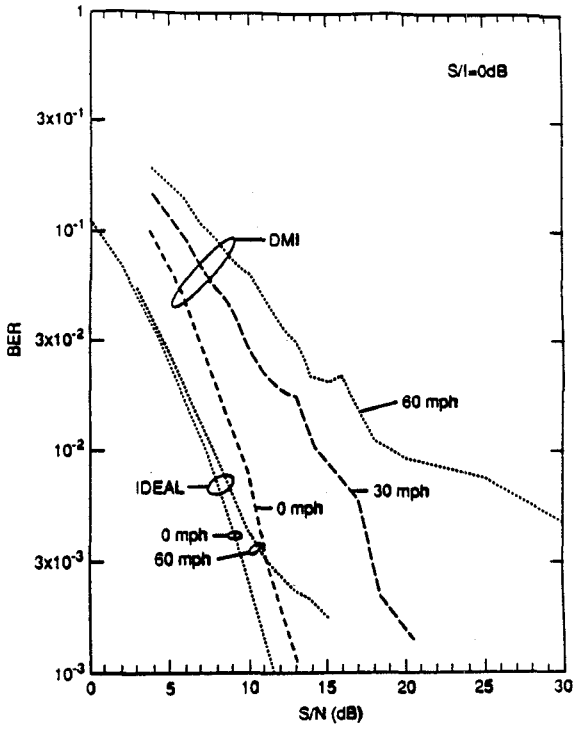

Fig. 3 BER versus S/N for DMI with an equal-power interferer.

As a further enhancement, consider the modification of DMI for the weights that maximize the SINR,

$$\mathbf{w}(k+1) = \hat{\mathbf{R}}_{i+n}^{-1}(k)\hat{\mathbf{r}}_{xd}^{*}(k) \quad , \quad (13)$$

where

$$\hat{\mathbf{R}}_{i+n}(k) = \frac{1}{K}\sum_{j=k-K+1}^{k}(\mathbf{x}(j)-\hat{\mathbf{r}}_{xd}(j)d^{*}(j))^{*} \cdot(\mathbf{x}(j)-\hat{\mathbf{r}}_{xd}(j)d^{*}(j))^{T} \quad (14)$$

which yields similar performance to (7) as verified by our computer simulation results. Now, with a single interferer (these techniques can also be extended to the multiple interferer case),

$$\mathbf{R}_{i+n} = \sigma^2\mathbf{I} + \mathbf{u}_1^{*}\mathbf{u}_1^{T} \quad (15)$$

and based on our previous discussion, for unequal weighting of noise and interference, our proposed subspace algorithm is given by

$$\mathbf{w}(k+1) = [\sigma^2\mathbf{I} + \beta\hat{\mathbf{u}}_1^{*}(k)\hat{\mathbf{u}}_1^{T}(k)]^{-1}\hat{\mathbf{r}}_{xd}^{*}(k) \quad . \quad (16)$$

Note the similarity to eigenanalysis [7].

Next, consider the problem of errors in the data-derived reference signal, where any symbol detection error made increases the subsequent weight estimation error. Since increased weight estimation error increases the BER, error propagation can occur, resulting in a complete loss of tracking. However, in IS-136, the 6 symbol CDVCC, located near the middle of each time slot, can be used to reduce the effect of error propagation. Recall from above that the CDVCC is known at the base station, so in principle it can be used as the reference signal for weight generation during the corresponding symbols of the time slot. However, it cannot be used directly because, as is the case with all data in the IS-136 time slot, the CDVCC symbols are encoded as differential phase shifts, rather than as coherent constellation points as required for the reference signal. We therefore use the detected phase of the data symbol prior to the CDVCC as the initial phase reference for CDVCC. This technique reduces the required S/N for a 10^{-2} BER about 1 dB for the case of an interferer with S/I = 0 dB.

Finally, consider the problem of channel variation over the estimation window. The adaptive array output signal (1) at the kth symbol is computed based on a uniform sliding window extending K symbols backward in time. The kth array output is then used to estimate the kth detected symbol $d(k)$, which is then used to compute the $k+1$th weight vector $\mathbf{w}(k+1)$, according to (7), and so on. Thus, the weights generated by (7) at symbol k are based on a received data vector $\mathbf{x}(k)$ which is time-centered about symbol $k-K/2$ (K assumed even). The kth weight vector is thus really more representative of the ideal weight vector in the middle of the window than at the end of the window. We cannot use this fact to improve the weight computation itself, because the weights depend on the $d(k)$, which are not available until the most recently computed array output is at hand. However, we can use it to produce a better signal for the purposes of data detection by the base station: Instead of driving the base station with the array output signal $y(k)$, we instead use a time-shifted version $z(k)$ that is computed based on the received data for which the weights more closely correspond, that is,

$$z(k) = \mathbf{w}^{T}(k+K/2)\mathbf{x}(k) \quad , \quad (17)$$

where, for notational simplicity, we have ignored the indexing issues that occur at the ends of the time slot. This technique also reduces the required S/N for a 10^{-2} BER about 1 dB for the case of an interferer with S/I = 0 dB.

Figure 4 shows the performance with an equal-power interferer with the combination of the algorithms discussed above. This combination includes time-shifted weights, use of CDVCC, and diagonal loading, with and without the subspace method, which we refer to as enhanced subspace and enhanced DMI, respectively. The tracking degradation at a 10^{-2} BER is reduced to about 1 dB at slow fading rates and 3 and 7 dB with the enhanced subspace and enhanced DMI methods, respectively, at 60 mph fading rates.

III. REAL-TIME ADAPTIVE ARRAY SYSTEM

The above techniques were implemented in our real-time four-antenna Adaptive Antenna Array (AAA) system, which is capable of both cellular-band IS-54 and PCS-band IS-136 operation. The basic system components are four I/Q receivers, a baseband processor, and a transmitter for remodulating the baseband array output signal back up to RF for use by the base station. The system is controlled and monitored from a networked workstation, using a customized graphical user interface (GUI) which permits real-time parameter changes and provides extensive performance-monitoring outputs.

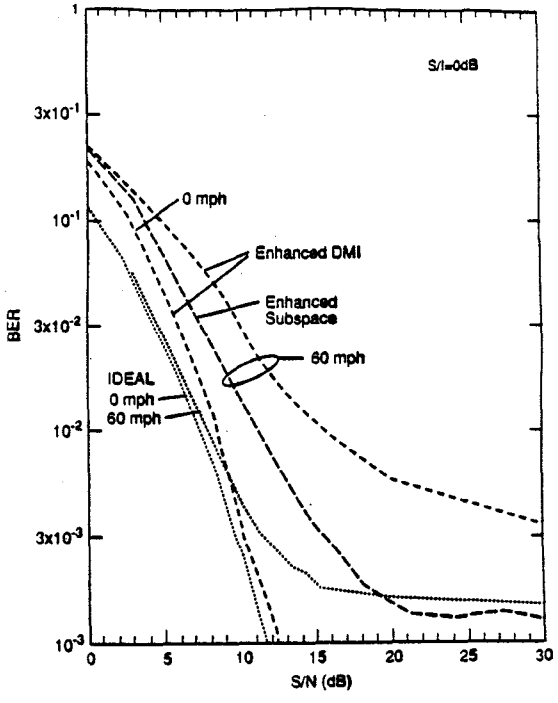

Fig. 4 BER versus S/N for the enhanced-tracking algorithms using a combination of techniques with an equal-power interferer.

The Baseband Processor performs all of the AAA signal processing functions described in this paper, and numerous ancillary functions in addition, as summarized below:

- **A/D sampling and conversion:** Rate $4/T$ = 97.2 ksamples/sec
- **Channel filtering:** Square root raised-cosine, α = 0.35.
- **DC compensation:** Mitigation of DC component independently on each subchannel, with user-selectable time constant.
- **Symbol timing estimation:** Determination of best timing epoch, within $T/8$ symbol of eye center.
- **Adaptive array processing:** User-selectable choices among basic algorithms and parameters: DMI/DL, MRC, slicing method (coherent or differential detection), adaptation stepsizes, diagonal augmentation, and frame timing adjustment. The implemented algorithm was equivalent to DMI with diagonal loading, using a user-selectable β and weight time shifting. Note that the use of CDVCC, the subspace method, and a variable β based on estimated I/N as described above, were not implemented. Furthermore, an exponential window (see [1]), rather than a rectangular window, was used.
- **Data logging:** Signal+noise+interference power on each subchannel is logged for later analysis, along with indications of special events such as A/D overloads.
- **Operational parameter monitoring:** Mean squared error, error vector magnitude display, selected timing epoch, weight trajectories, signal powers and more are available (remotely) at the workstation GUI in quasi-real-time.

IV. EXPERIMENTAL RESULTS

The real-time experimental results in this paper were derived using our AAA real-time system with an RF multipath fading channel emulator under laboratory conditions in order to provide repeatable results. The multipath emulator can produce four independent channels with three paths each to support co-channel interference testing with one or two interferers, with Doppler rates up to 740 Hz and delay spreads up to 100 μs, and with Rayleigh, Rician, or log-normal fading.

The configuration shown in Figure 5 was used for BER versus S/N and signal-to-interference ratio testing in fading conditions. This testing provided the data needed to verify our simulation results.

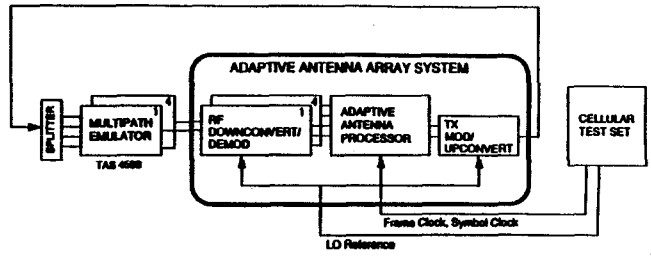

Fig. 5 Block diagram of TDMA/IS-136 laboratory testbed for BER testing with the multipath emulator.

Figures 6 and 7 compare the experimental results using the laboratory RF multipath emulator with the computer simulation results. These results are for DMI with weight time shifting and diagonal loading with a β fixed for each figure: β = 1 (MRC) in Figure 6, and β = 0.43 (optimum β for I/N = 10 dB) in Figure 7. (Note that the experimental algorithm differs from the simulation algorithm in the use of an exponential rather than a rectangular window to reduce computational complexity. Our simulation results indicate that this should have a negligible effect on the results, however.) There is good agreement between the experimental and computer simulation results, except for the case of an equal-power interferer at 184 Hz fading. In this case, the experimental system has a higher BER, probably due to the significant additional ISI power induced by an equal-power interferer. This ISI is due primarily

to analog filtering effects which are not modeled in the simulations.

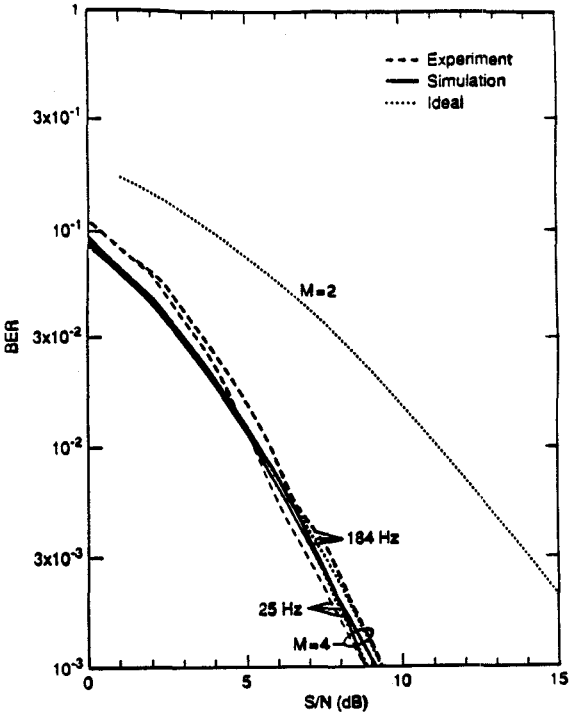

Fig. 6 BER versus S/N for the enhanced DMI algorithm with noise only - comparison of experimental and computer simulation results.

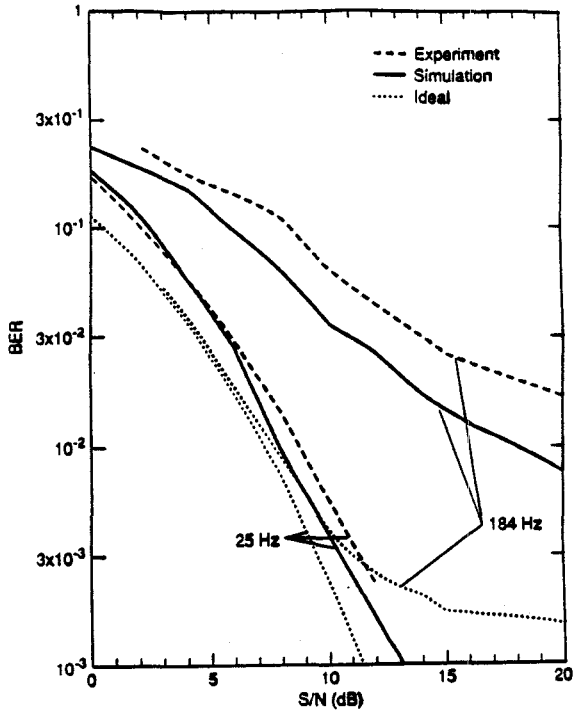

Fig. 7 BER versus S/N for the enhanced DMI algorithm with an equal-power interferer - comparison of experimental and computer simulation results.

Finally, based on the results of Section II, we note that we should be able to achieve even better performance in our experimental system (when interference is present) by using CDVCC, diagonal loading with β based on estimated I/N, and/or the subspace method, at the cost of increased computational complexity.

V. CONCLUSIONS

In this memorandum we have described the implementation of a prototype four-element adaptive antenna array for IS-136 base stations. Experimental results using our enhanced adaptive array algorithm for range extension showed that we could achieve more than 5 dB of the theoretical 6 dB higher gain at a 10^{-2} BER in a Rayleigh fading environment than a two-element array using postdetection diversity combining. This corresponds to a 40% increase in range in a typical mobile radio environment. At slow speeds in the presence of interference, the four-element array realized more than 3 dB of the theoretical 4 dB gain advantage relative to a two-element array in the absence of interference, even with a cochannel interferer having the same average received signal power as the desired signal. At 60 mph fading rates, the results show that an interferer can reach nearly the level of the desired signal while maintaining a 10^{-2} BER. This indicates the feasibility of increased capacity through higher frequency reuse, perhaps even including the possibility of frequency reuse within a cell. Thus, we have demonstrated that adaptive arrays can increase both the range and capacity of TDMA cellular systems.

ACKNOWLEDGEMENTS

We gratefully acknowledge useful discussions on eigenanalysis with A. Haimovich.

REFERENCES

[1] J. H. Winters, "Signal Acquisition and Tracking with Adaptive Arrays in the Digital Mobile Radio System IS-54 with Flat Fading," *IEEE Trans. on Vehicular Technology*, November 1993.

[2] G. E. Bottomley and K. Jamal, "Adaptive arrays and MLSE equalization," *Proc. of the Vehicular Technology Conference*, Chicago, IL, June 25-28, 1995, pp. 50-54.

[3] K. J. Molnar and G. E. Bottomley, "D-AMPS performance in PCS bands with array processing," *Proc. of the Vehicular Technology Conference*, Atlanta, GA, April 28 - May 1, 1996, pp. 1496-1500.

[4] R. A. Monzingo and T. W. Miller, *Introduction to Adaptive Arrays*, John Wiley and Sons, New York, 1980.

[5] D. J. Goodman, "Trends in cellular and cordless communications," *IEEE Communications Magazine*, vol. 29, June 1991, pp. 31-40.

[6] J. C. Nash, *Compact Numerical Methods for Computers*, 2nd edition, Adam Hilger, Bristol and New York, p. 121.

[7] A. Haimovich and X. Wu, "Eigenanalysis based array processing for mobile communications," in *Proceedings of the 1994 Princeton Conference on Information, Science, and Systems*, Princeton, NJ, March 1994, pp. 203-208.